Indian J. Met. Hydrol. Geophys. (1978), 29, 4, 643-654

551·511 (267) '1973'

A study of the atmospheric boundary layer over the Arabian Sea from ISMEX-1973 data

Y. RAMANATHAN

Meteorological Office, New Delhi

(*Received 23 June 1977*)

ABSTRACT. The ISMEX-73 data was studied to assess the bulk layer variations in the Arabian Sea along 10°N and along the equator. It was found that: (*i*) Along the equator the friction velocities were low both during May and June 1973, indicating the predominance of the buoyancy effects; (*ii*) There were practically no inversions along the equator; (*iii*) During May, buoyancy effects were dominant with low friction velocities along 10°N also. But in June forced convection became significant with the increase of friction velocities; (*iv*) Inversions were observed along 10°N. The base was observed at higher elevations with weaker inversion strength downstreams from 50°E to 70° E; (*v*) Mixed layers were generally unsaturated in both the sections; (*vi*) Sea surface virtual temperatures were mostly higher than virtual air temperatures in both the sections; (*vii*) The drag coefficients were of the order of 1×10^{-3}; (*viii*) During a spell of rainfall activity over India, computations at a stationary site at 10° N, 60·2° E showed high values of positive sea-air temperature differences, generally saturated mixed layers, no inversions, high specific humidity content; (*ix*) During a spell of weak rainfall activity over India, however, the computations at the same location showed low sea-air temperature difference (often negative), enhanced wind speed, lower sea-surface temperatures, unsaturated mixed layers and daily inversions.

1. Introduction

It is well known that the energy of the major rain-producing systems in the tropics like the monsoon and the tropical cyclones, is largely derived from the air-sea exchanges of heat, moisture and momentum in the atmospheric boundary layer. One of the objectives of the Global Atmospheric Research Programme (GARP) and its sub-programme MONEX-1978-79 is the understanding of the boundary layer processes for realistic parameterization and incorporation in the forecast and simulation models for the tropics. Reliable measurements to obtain representative values of the energy flux have been planned from ship-board, aircraft and buoys. During the International Indian Ocean Expedition, 1963-65, boundary layer measurements were made by Bunker (1965). He found that the sensible heat transport was downward above 1·5 km over the west Arabian Sea and upward over the east Arabian Sea. He also estimated the transport of moisture at heights upto 600 mb. A few studies based on the data of the Indo-Soviet Meteorological Expedition (ISMEX) 1973 sought to confirm some of the earlier findings. Jambunathan and Ramamurthy (1975) discussed the sea and air temperature distributions over the Arabian Sea. They found a low-level inversion over the west Arabian Sea during May-June 1973. Pant (1978) discussed the vertical structure of the atmospheric boundary layer in the west Indian Ocean. He found a mixed layer whose eight varied from 200 m and less off north Africa and the Arabian coast to about 600 m near 60°E. The present study from ISMEX-73 data is somewhat more detailed, and based on the available radiosonde/radiowind, sea-surface and anemometer level observations along 10° N and along the equator taken on board the U.S.S.R. research vessles, *Slokalaisky* and *Okean*, from 18 May to 4 July 1973. Though the conventional upper air data is not specially designed for boundary layer studies, the method devised by Deardorff (1972 b) could be used for bulk layer estimates of the boundary layer variables. The scheme was adopted by Moss and Rosenthal (1975) to compute the exchange and drag coefficients from the upper air data in respect of the hurricanes (Daisy 1958 and Inez 1966). The computations agreed remarkably well with those calculated by budget methods. Section 2 contains details of Deardorff's method relevant to the present study. Section 3 gives details of the arrangement of data and the computations. The results are discussed in Section 4. Inversion statistics are presented in Section 5. A summary and conclusions are given in the last section.

2. Method of computation

2·1. *Basis of Deardorff's scheme*

The planetary boundary layer (PBL) is the region of the atmosphere where the influence of the underlying ocean/land surface on the atmospheric

flow is felt through turbulent exchanges of momentum heat and moisture. The depth of the PBL is of the orders of 1 to 2 km. The observed main subdivisions are as follows :

(*a*) The surface layer $\sim$ 100 m with an super adiabatic temperature gradient and decrease of specific humidity (q) with height, resulting in a slight statical instability. The turbulent fluxes do not deviate from the surface values by more than 20%. The pressure and coriolis forces are neglected compared to the divergence of the turbulent fluxes.

(*b*) The neutral stratified mixed layer up to about 950 mb which is adiabatic but has a constant specific humidity.

(*c*) The transition layer whose thickness is $\sim$100 m and whose top coincides with the lifting condensation level (LCL). This layer separates the cloud convection regime above from the regime of dry convection and mechanical mixing below.

(*d*) The cloud layer extending from the top of the transition layer to the base of the inversion. The temperature gradient is slightly stronger than moist-adiabatic lapse-rate. Specific humidity decreases weakly upward.

This is the conventional picture of a tradewind boundary layer (Augstein *et al.* 1974) and the cases considered in this study confirmed broadly to the above classification. In some cases, however, the transition layer was absent. Deardorff (1972 b) developed the method for parameterizing all aspects of the PBL in a general circulation model where the PBL cannot be represented by many levels. The treatment is based on the similarity theory (Monin and Oboukhov 1954). The assumption is that in the constant flux surface layer (inner layer) the mean variables depend upon surface fluxes or characteristics but not upon the mean variables for the mixed layer, while differences or deficits between mean variables at the top of the surface layer and at the top of the PBL still depend on the surface fluxes but not on the surface characteristics. The mean variables under consideration are averages of the horizontal wind components u and v (x-axis along the mean wind direction in the lower surface layer), specific humidity (q) and the virtual potential temperature ($\theta_v = \theta + 0{\cdot}61q$). The surface influx is the stress in the downstream x-direction, $\tau_s = \rho_s u_*^2$ (u_* is the friction velocity), the virtual sensible heat flux relative to θ_v, $H_s = \rho_s c_p \overline{(w'\theta_v')}$ and the moisture flux $E_s = \rho_s \overline{(w'q')}_a$ at the anemometer level, where w is the instantaneous vertical velocity and the primes are the fluctuations from the mean (denoted by a overbar). The surface characteristics are the roughness length z_0, θ_{vs}, q_s for the sea-surface. Two important length scales are involved. The first is the Monin-Oboukhov length L.

$$L = -u_*^3 \Big/ \left(k \frac{g}{\theta_{vm}} \frac{H_s}{c_p \rho_s} \right)$$

where k is the Von-Karman constant (=0·35) and θ_{vm} is the average for the mixed layer whose height is h. L arises from the ratio of the two production terms in the turbulent kinetic energy equation $-\overline{u'w'}\,(\partial u/\partial z)$ and $-\overline{w'\theta_v'}\,(g/\theta_{vm})$ which are the Reynolds stress and the buoyancy flux respectively.

$$(i.e.)\quad u_*^2 \frac{\partial u}{\partial z} : \frac{g}{\rho_s} \frac{H_s}{c_p \theta_{vm}}$$

where $\partial u/\partial z \sim u_*/z$ near the surface. L then represents the height where the magnitudes of these two terms are of the same order. At depths $h << L$, the turbulent energy balance is maintained predominantly by Reynolds stresses and the buoyancy flux plays only a minor role. This is the forced convection or wind-dominated regime in contrast to the free convection or heat-dominated regime. The surface layer parameters u, θ_v, q rendered dimensionless by u_* are believed to be functions of $(z_a - z_s)/z_0$ and $(z_a - z_s)/L$ where z_a is the anemometer level ($\sim$ 10m) and z_s is the height of the surface which is zero over the ocean. In the part of the PBL above the surface, the dimensionless velocity and temperature defects are also believed to be functions of $(h - z_s)/z$ and $(h - z_s)/z_0$. The universal function for the surface layer is based on the formulations of Businger (1966) and Businger *et al.* (1971) from the Kansas experimental data. The deficit function used to depict processes in the remainder of the PBL is based on Deardorff's numerical simulations (1970 a and 1970 b and 1972 a).

2·2. *Depth of the PBL*

In the standard similarity theory for a stationary and horizontally homogeneous PBL, the Ekman depth $\lambda_E = ku_d/|f|$ where f is the coriolis parameter, is used as the length scale. This formulation is unsuitable for applications closer to the equator. For cases when $H_s > 0$ the time-dependent actual height h is used as the PBL height (Zilitinkevich and Deardorff 1974). In the hurricane cases, Moss and Rosenthal (1975)

reasonably assumed the top of the PBL, as the lifting condensation level (LCL), thereby having a saturated sub-cloud mixing layer. As the presence of cumulus activity was not widespread in the cases studied, this blanket assumption would not have been realistic. Also there were many cases with no inversions for using inversion base. In this study h was determined on the lines suggested by Melgarejo and Deardorff (1974). For this the thermal stability of the PBL was first determined as :

$$\left.\begin{matrix}\text{Unstable}\\ \text{Stable}\\ \text{Neutral}\end{matrix}\right\} \text{ if } \quad (\theta_{vs} - \theta_{va}) \begin{matrix}>\\<\\=\end{matrix} 0 \qquad (2.2.1)$$

In all the cases the vertical profiles of θ_v and q were examined upto a height of 2 km. In the unstable/neutral cases the relative constancy of both within a region $z<h$ as compared to $z>h$ which was believed to correspond to the level where the heat, moisture and momentum fluxes due to turbulence approached zero rapidly above the height. In the stable cases, the height of the low level wind maximum in u profile was taken as h. In some cases the v profile was also used if there was a better defined maximum.

2.3. *Exchange coefficients*

The equations from Deardorff (1972 b) relevant to the computations in this study are now presented. A Bulk Richardson Number :

$$R_{IB} = g\,(h - z_s)\,(\theta_{vm} - \theta_{vs}) \,/\, \theta_{vm}\, u_m^2 \qquad (2.3.1)$$

is first computed where z_s is the height of the surface which is zero over the ocean, and $z_u \sim 10$ m is the anemometer level. For the unstable case where $R_{IB} < 0$, the bulk momentum transfer coefficient :

$$C_u = \left[C_{uN}^{-1} - 25 \exp\,(0{\cdot}06\,\xi - 0{\cdot}03\,\xi^2) \right] \qquad (2{\cdot}3{\cdot}2)$$

and the bulk heat transfer coefficient :

$$C_\theta = \left[C_{\theta N}^{-1} + C_u^{-1} - C_{uN} \right]^{-1} \qquad (2.3.3)$$

where $\xi = \log_{10}(-R_{IB}) - 3.5 \qquad (2.3.4)$

and the neutral values :

$$C_{uN} = \left[k^{-1} \log_e \left\{ \frac{0.025\,h}{z_0} \right\} + 8.1 \right]^{-1} \qquad (2.3.5)$$

$$C_{\theta N} = \left[k^{-1}\, 0.74 \log_e \left\{ \frac{0.025\,h}{z_0} \right\} + 7.3 \right]^{-1} \qquad (2.3.6)$$

for the stable case ($R_{IB}>0$) :

$$C_u = C_{uN}\,(1 - R_{IB}/3{\cdot}05) \qquad (2.3.7)$$

$$C_\theta = C_{\theta N}\,(1 - R_{IB}/3{\cdot}05) \qquad (2.3.8)$$

The friction velocity :

$$u_* = C_u \cdot u_m \qquad (2.3.9)$$

and the eddy flux of virtual potential temperature at the anemometer level :

$$(-\overline{w'\theta_v'})_a = C_\theta\, u_*\, (\theta_{vm} - \theta_{vs}) \qquad (2.3.10)$$

The anemometer level momentum transfer coefficient :

$$C_{ua} = u_*\, u_a \qquad (2.3.11)$$

where u_a is the anemometer level u value.

Similarly the anemometer level heat transfer coefficient :

$$C_{\theta a} = \overline{(-w'\,\theta_v')}_a \,/\, u_*\,(\theta_{vm} - \theta_{va}) \qquad (2.3.12)$$

The drag coefficient :

$$C_{da} = C_{ua}^2 \qquad (2.3.13)$$

The heat exchange coefficient :

$$C_{Ha} = C_{ua} \cdot C_{\theta a} \qquad (2.3.14)$$

If z_0 is the roughness parameter and is known, the set of equations (2.3.1) to (2.3.14) represent a complete set for deriving the bulk layer estimates of the transfer coefficients. The values of z_0 over the oceans especially at high wind speeds is very uncertain. Charnock (1955) suggested on dimensional grounds the relation :

$$z_0 = B_0\, u_*^2/g \qquad (2.3.15)$$

where B_0 is a numerical constant. Kitaigorodskii and Volkov (1965) suggested a value of 0·035 for B_0 which has been used in this study. The system of equations (2.3.1) to (2.3.15) are solved implicitly starting from a value for z_0=0·025 cm and the estimates for R_{IB}, u_*, C_{ua}, $C_{\theta a}$, C_{da}, C_{Ha} were obtained.

The Monin-Oboukhov length was computed from :

$$L = C_u^2 h / k C_\theta\, (R_{IB}) \qquad (2.3.16)$$

3. Data and computation

3.1. *Data source*

Four oceanographic research vessels from the USSR participated in ISMEX-73 during May-July, 1973. A total of 124 radiosonde/radiowind, sea-surface and anemometer level observations of temperature, wind and humidity from the ships *Shokalaisky* and *Okean* (Figs. 1 and 2) along

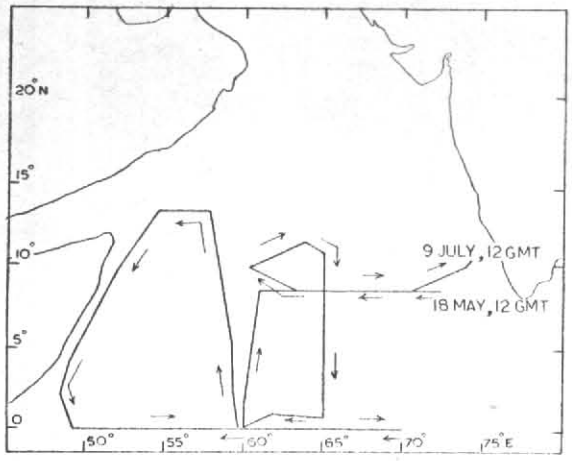

Fig. 4. *Okean* cruise, 18 May, 12 GMT to 9 July, 12 GMT

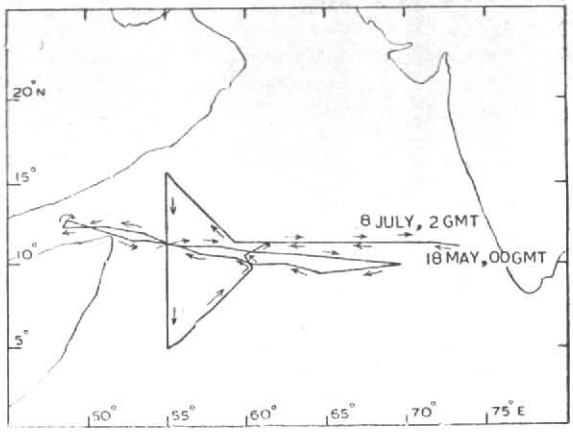

Fig. 2. *Shokalaisky* cruise 18 May, 00 GMT to 08 July, 12 GMT

10°N and along the equator in the Arabian Sea were the data source. The period of observations, which was not always continuous, was from 15 May to 7 July 1973. Besides, the ship *Shokalaisky* took observations at a stationary site at 10°N, 60·2°E in two spells I nad II from 1 June 1973 to 7 June 1973 and again from 27 June 1973 to 4 July 1973.

3.2. *Synoptic situation over India*

The monsoon set in, in the Kerala coast in the southwest India by 4 June 1973 and advanced upto central and northwest India by 13 June 1973. There was a lull in the rainfall activity over India during the remaining days in June 1973 and till 4 July 1973 when the rainfall activity once again revived (Jambunathan and Ramamurthy 1974). The two spells I and II of the stationary observations broadly coincided with these periods of active and deficient rainfall over India.

3.3. *Computations*

Computation of parameters listed in Table 1 were made as discussed in section 2.3 for all the ascents. The computations were then grouped into longitudinal sections centred around 50°E, 55°E, 60°E, 65°E, 70°E and 75°E. The averages for the months May and June (the few days in July added) for the parameters were then worked out. The cases were predominantly (94 out of 124 ascents) unstable ($\theta_{vs} > \theta_{vm}$) atmosphere. The stable cases were mostly in June at 60°E and at 55°E. The Figs. 3-14 and the discussion on the averages are representatitive of unstable cases. However, day to day variations at the stationary site 10°N, 60·2°E are discussed in respect of both the stable and unstable cases

TABLE 1

Parameter	Symbol	Units	Order
Mixed layer height, roughness length	h/z	—	10^3 to 10^7
Monin-Oboukhov length	L	metres	1 to 10^3
Mixed layer height	h	metres	10^2 to 10^3
Lifting condensation level	LCL	metres	10^2
Drag coefficient at anemometer level	C_{da}	—	10^{-3}
Heat transfer coefficient at anemometer level	$C_{\theta a}$	—	10^{-3}
Momentum transfer coefficient at anemometer level	C_{vd}	—	10^{-3}
Anemometer level scale height	h/L	—	1 to 10^2
Sea surface virtual temperature	θ_{vs}	°K	10^2
Anemometer level virtual air temperature	θva	°K	10^2
Mean virtual air temperature for atmospheric mixed layer	θvm	°K	10^2
Specific humidity	q	gm/kgm	10
Bulk Richardson No.	R_{IB}	—	−3 to +3
Atmospheric mixed layer mean zonal velocity with respect to surface wind direction	u_m	m sec^{-1}	1 to 10
Friction velocity in the air	u_*	cm	1 to 10
Friction velocity in water	w_*	cm	1

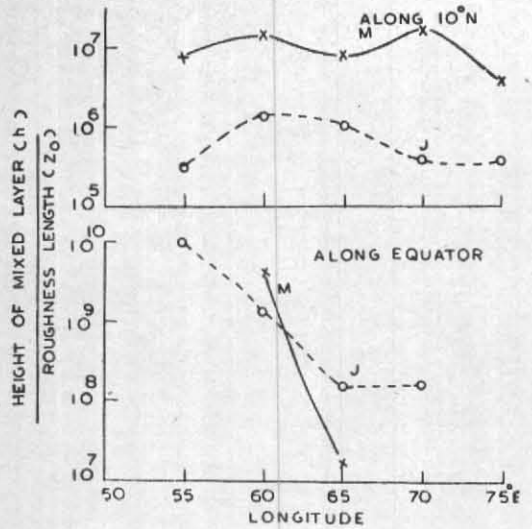

Fig. 3

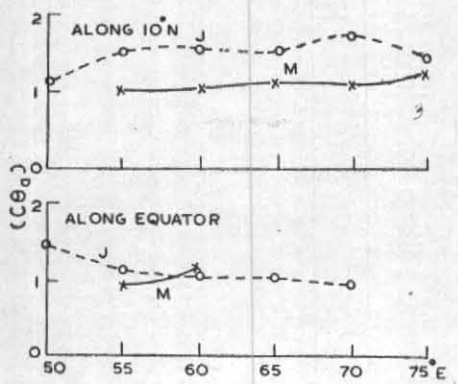

Fig. 5

for both the spells I and II. The data distribution was not homogeneous in the sections and were concentrated more in the sections around 60°E and 65°E. Continuous lines in the diagrams (3-16) represent the May variations and the dotted lines indicate the variations in June.

4. Discussion of the results

4·1. *Averages for longitudinal cross-sections*

4·1·1. In Fig. 3 the scale parameter h/z_0 shows increase at all the sections from May to June. This is partly due to the decrease of the mixed layer height h (Fig. 4) due to to less unstable conditions of the atmosphere and increase of the roughness parameter z_0 due to increase of u_m *and* u_*. The values of h/z_0 exceed 10^3 in all the cases and hence are within the valid range for the application of the Businger-Dyer type formulation for the surface layer.

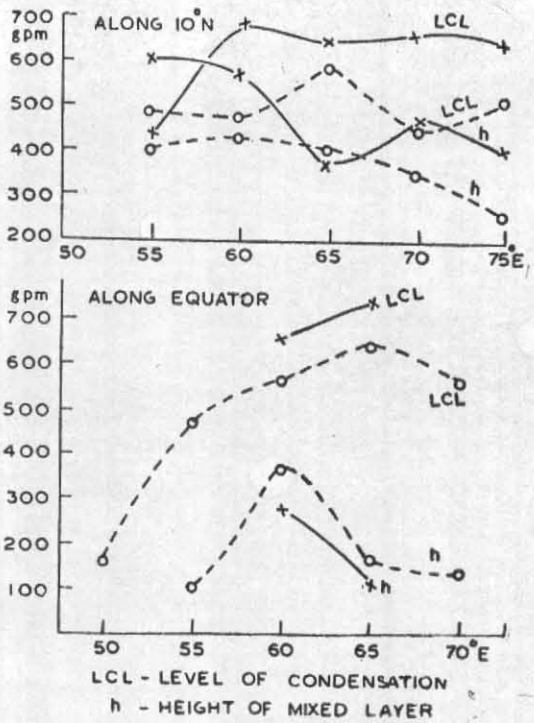

Fig. 4

4·1·2. The LCL was generally higher than h in all the sections both along 10°N and along the equator in both the months. This indicated that the mixed layers were generally unsaturated. The values in the equatorial section showed that the mixed layers were relatively dry compared to those along 10°N. Except at 65°E the mixed layer was more wet along 10°N in June than in May. But h values were lower in June perhaps due to suppressed convective activity.

4·1·3. L values were one order less than h values in both the months along the equator, thereby implying that the buoyancy effects were more dominant than the Reynolds stresses in the production (destruction) of turbulent kinetic energy (Figs. 7 & 8). This was the case along 10°N also in May. But in the June, L values were of the same order as h values. The classification of the data monthwise appeared to be the same as L-wise. The turbulent energy balance was now maintained both by the buoyancy effects and the Reynolds stresses. In the surface layer the Reynolds stresses were more prominent in a forced convection regime.

4·1·4. The virtual sea-surface temperatures (θ_{vs}) were higher than the mean air virtual temperatures (θ_{va}) for the bulk mixed layer in 94 out of 124 cases. The discussion hence relates to these unstable cases (Fig. 9). θ_{vs} values were 1.5

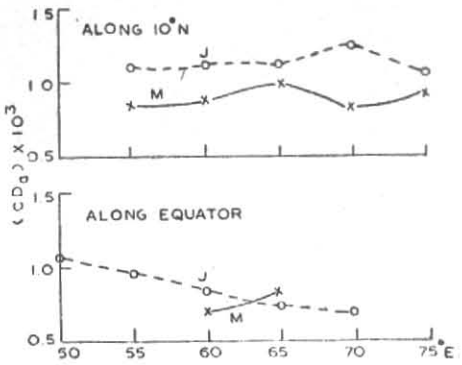

Fig. 6

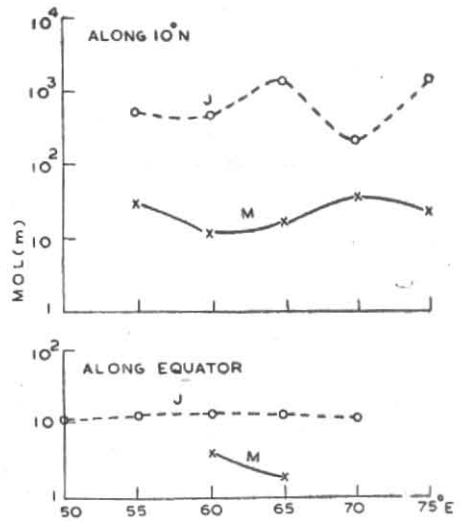

Fig. 7. Monin Oboukhov length (metres) [MOL]

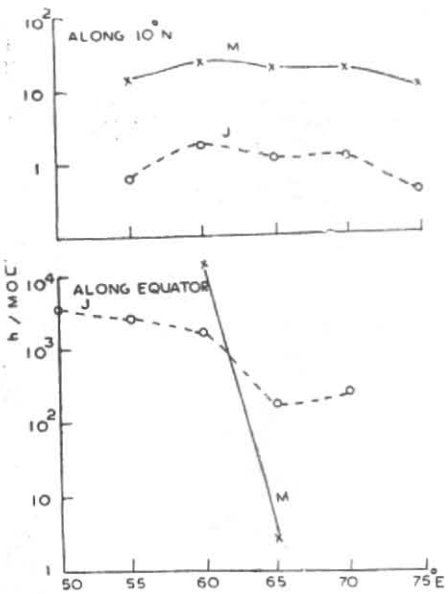

Fig. 8. Ratio h/MOL

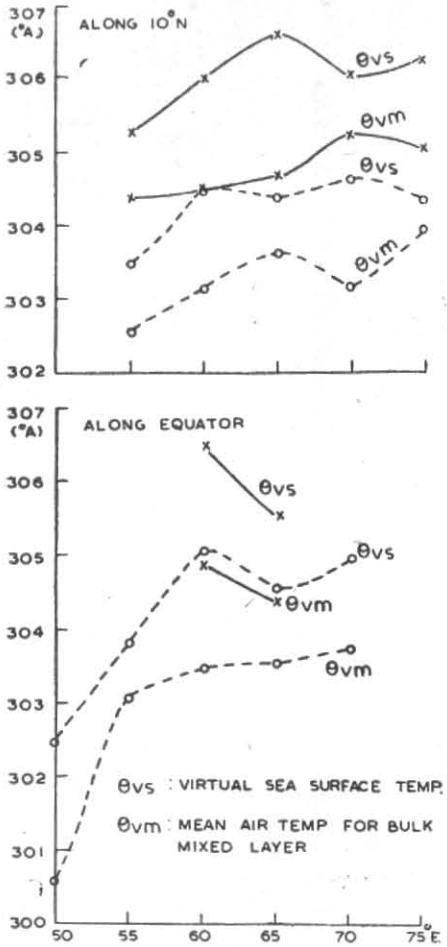

Fig. 9

to 2°C higher in May than June both along 10°N and along the equator. The specific humidity values were, however, more or less the same (18 to 20 gm/kgm — Fig. 10). These values are much higher than observed over the trades in the Atlantic (Roll 1965).

4.1.5. The R_{IB} profiles (Fig. 11) show near neutral stability conditions in June in consistent with the large L values for a forced convection regime along 10°N. Markedly unstable conditions prevailed along 10°N, 60·2°E in May. Profiles for the equatorial sector show unstable conditions with high values for 55°E and 70°E in June.

4.1.6. The mean u_m values for the mixed layers were below 5 m/sec^{-1} for May and June over the equator and for May along 10°N (Fig. 12). In June the values were more than 10 m sec^{-1} along 10°N with a peak 15 m/sec at 65°E. The effect of the increase in June could be seen in the friction velocity u_* values (Fig. 13), the peak being 51 cm along 65°E, 10°N.

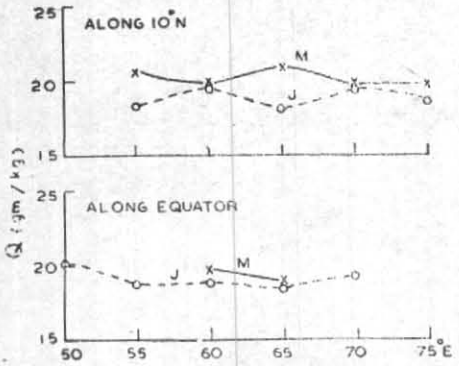

Fig. 10. Specific humidity Q (gm/kgm)

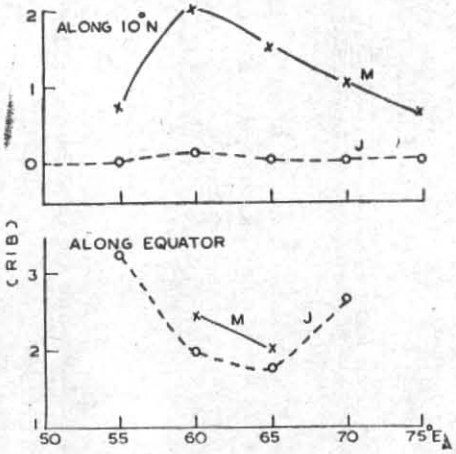

Fig. 11. Bulk Richardson's No. (R_{IB})

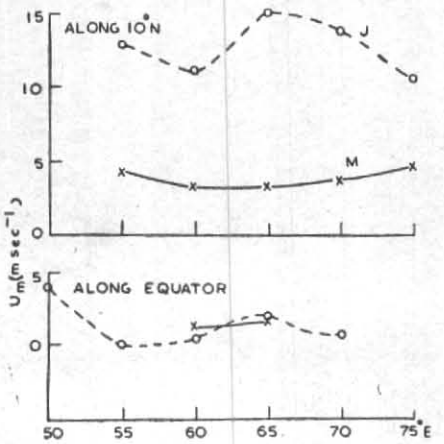

Fig. 12. Mean u values for mixed layers (u_m) m/sec

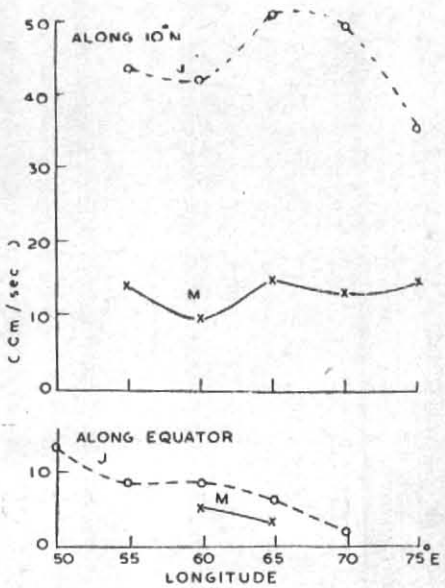

Fig. 13. Friction velocity u_* (cm/sec)

4.1.7. Figs. 5, 6 and 14 show respectively the anemometer level drag coefficient C_{da}, heat transfer coefficient $C_{\theta a}$, and the momentum transfer coefficient C_{va}. $C_{\theta a}$ values were higher than C_{da} values. The June values along 10°N were higher for May in consistent with increased wind speed. The highest values of $C_{\theta a}$ ($1{\cdot}7\times10^{-3}$) and C_{da} ($1{\cdot}27\times10^{-3}$) were higher than the values over the equator. Pond *et al.* (1974) reported C_{da} values ($1{\cdot}55\pm0{\cdot}28$) for the Arabian Sea which are of the same order as the C_{da} values obtained in this study.

4.2. At the stationary location, 10°N, 60·2°E; Figs. 15 and 16 present the day to day variations of the parameters at the stationary location (10°N, 60·2°E) in the spells I and II corresponding to the periods of active rainfall and weak rainfall over India.

4.2.1. Fig. 15 (a) shows the significant positive sea-air temperature difference ($\theta_{vs}-\theta_{vm}$). During the spell I the atmosphere was unstable with respect to θ_{vs} values which were considerably higher than θ_{vm} values, the average being 1·9° with the maximum of 3·1° on 3 June 1973. The variability of θ_{vs} was very little on a day to day basis during the spell I. There were significant variations in θ_{va} values perhaps due to evaporative cooling. In contrast θ_{vs} values in the spell II were less than the spell I values by about 2°. Also the air temperatures (θ_{va}) were higher or closer to θ_{vs} values. Stable conditions prevailed on many occasions. This would represent a rate of turbulent kinetic energy loss by working agains the buoyancy gradient and increasing the potential energy of the mean field of density. The increase in u_* values no doubt showed increase of production of turbulent kine-

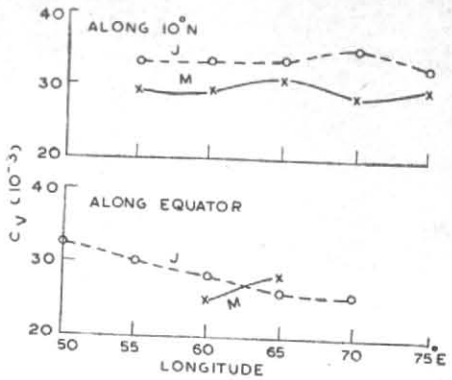

Fig. 14. Anemometer momentum transfer coefficient C_v ($\times 10^{-3}$)

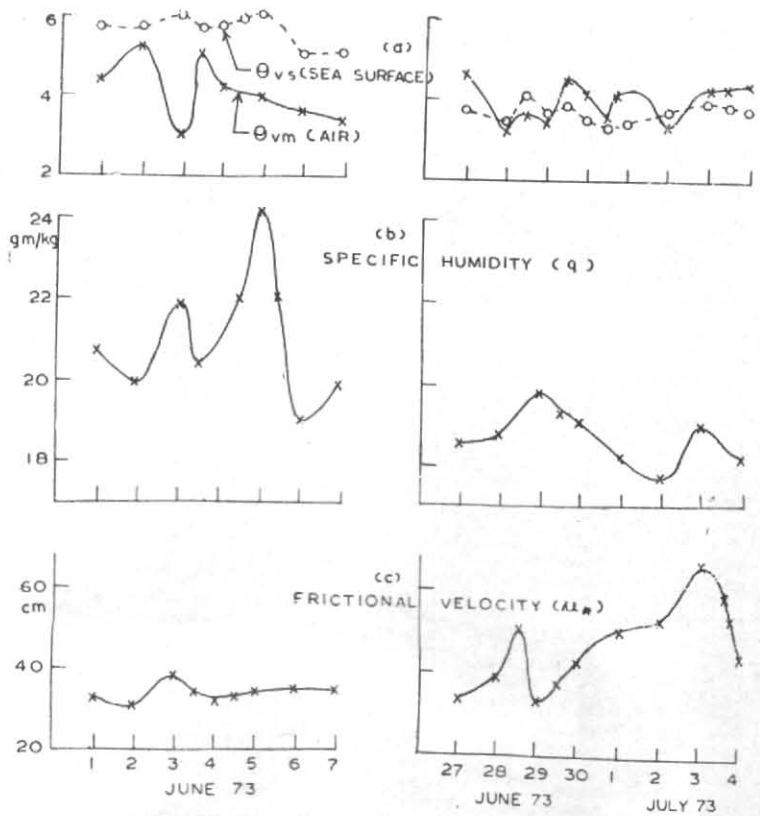

Fig. 15. At stationary location 10°N, 60·2°E

tic energy by mechanical processes, but since the buoyant effect was destructive, the turbulent activity was low.

4·2·2. The specific humidity (q) values were over 19 gm/kgm (Fig. 15 b) with a maximum of 24·2 gm/kgm on 5 June in the spell I. In the spell II, q values were all less than 20 gm/kgm consistent with low turbulent activity.

4·2·3. The scale parameter h/z_0 values in the spell II were somewhat lower than those in the spell I due to increased z_0 arising out of larger u_* values and decreased h values due to suppressed convection.

4·2·4. The heights of the mixed layer (h) were lower than the LCL values generally in the spell II. In the spell I, h values exceeded the LCL values from 4 June, which was incidentally the date of onset of monsoon over India. This indicated stepping up of convective activity and saturation of the mixed layers.

4·2·5. The Monin-Oboukhov length (L) values were larger numerically in the spell II than those in spell I. But they were alternating between

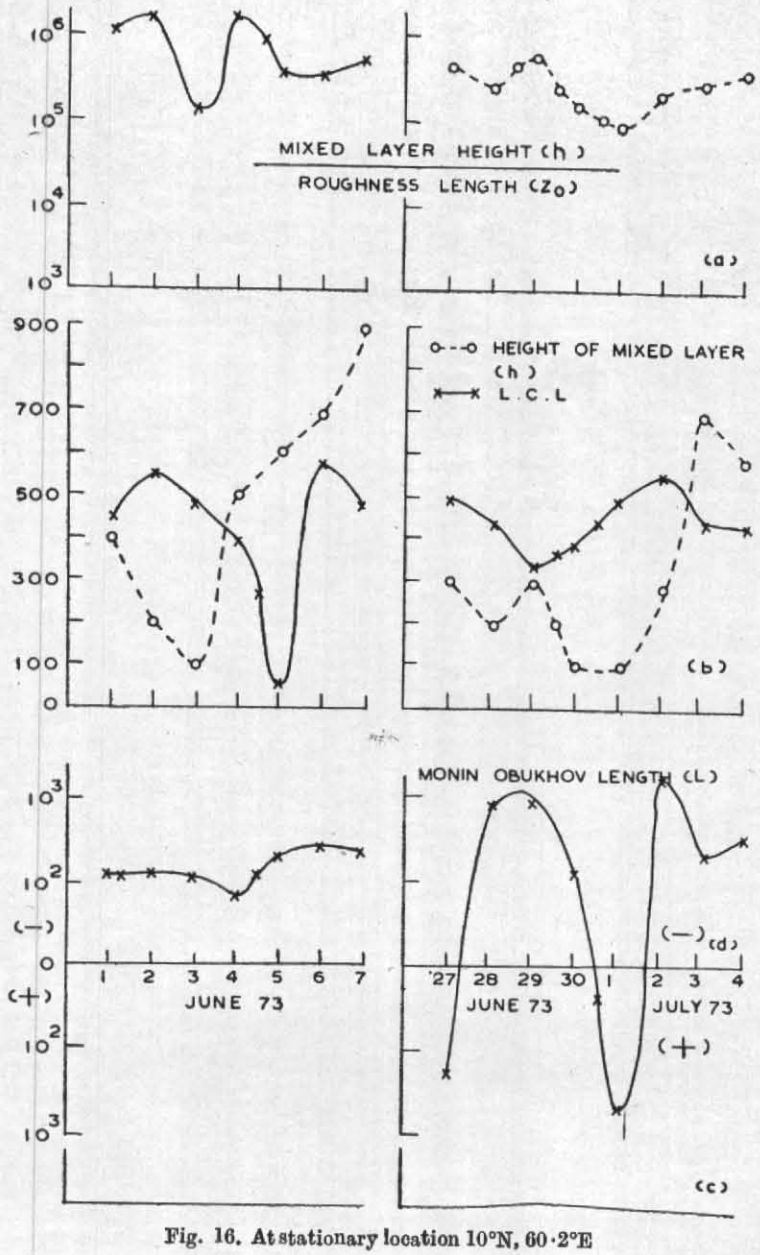

Fig. 16. At stationary location 10°N, 60·2°E

positive and negative values in spell II corresponding to stable and unstable conditions, whereas they were all negative in spell I corresponding to unstable conditions.

5. Inversion statistics

The inversion layer details are presented in Table 2.

5·1. *Along the equator*

Of the 41 available cases, 39 were unstable cases with $\theta_{vs} > \theta_{vm}$. In these, there were only two cases of inversion in the dry bulb temperature profiles, at a mean height of 1625 m with an inversion strength of 0·6°. The values increased above the mixed layer but the inversion was practically absent. Similar observations of the absence of inversions at the equator have been reported by Augstein *et al.* (1974) from the data of METEOR at the equator near 30°W. With low u_* values, mixing by free convection must be responsible for weakening the layered structure.

5·2. *Along 10°N*

Out of 83 cases (Table 2) 30 inversions were observed. Stable conditions ($\theta_{vm} > \theta_{vs}$) prevailed in 16 cases and unstable conditions ($\theta_{vs} > \theta_{vm}$) in 14 cases. During May when relatively

TABLE 2

Inversion layer details

	a	b	c	d	e	a	b	c	d	e	a	b	c	d	e
			50°E					55°E					60°E		
1	—	—	—	—	—	—	—	—	—	—	—	—	—	—	—
2	—	—	—	—	—	—	—	—	—	—	—	—	—	—	—
3	—	—	—	—	—	—	—	—	—	—	9	—	—	—	—
4	—	—	—	—	—	1	1	990	160	1·0	3	1	920	80	I
5	1	—	—	—	—	1	—	—	—	—	—	—	—	—	—
6	2	2	350	280	1·1	8	4	662	411	2·1	15	7	1713	244	1·2
7	1	—	—	—	—	1	—	—	—	—	22	2	1625	265	0·6
8	2	1	200	200	1·3	2	2	735	305	1·7	21	9	1262	200	1·5
			65°E					70°E					75°E		
1	—	—	—	—	—	—	—	—	—	—	—	—	—	—	—
2	1	1	1860	190	I	—	—	—	—	—	—	—	—	—	—
3	1	—	—	—	—	—	—	—	—	—	—	—	—	—	—
4	6	—	—	—	—	5	2	1185	390	0·6	1	—	—	—	—
5	—	—	—	—	—	—	—	—	—	—	—	—	—	—	—
6	1	1	960	340	1·0	1	1	1950	50	0·4	—	—	—	—	—
7	2	—	—	—	—	3	—	—	—	—	—	—	—	—	—
8	8	2	1470	280	2·1	4	—	—	—	—	2	—	—	—	—

(a) Total number of cases (124; 30 stable and 94 unstable cases) (b) Number of inversions
(c) Base of inversion in metres (d) Thickness of inversion in metres
(e) Temperature increase in °C (I-Isothermal)

1. Stable cases along the equator in May
2. Stable cases along 10°N in May
3. Unstable cases along the equator in May
4. Unstable cases along 10°N in May
5. Stable cases along the equator in June
6. Stable cases along 10°N in June
7. Unstable cases along the equator in June
8. Unstable cases along 10° N in June

lower u_* values were observed and the L values indicated more buoyancy producing turbulent kinetic energy, 5 cases of inversion out of a total of 17 cases were observed. During June with enhanced u_* and L values, 29 inversions were observed out of a total of 66 cases. It may also be pointed out that there were 27 cases of stable conditions ($\theta_{vm} > \theta_{vs}$) in June. Though the data coverage was not homogeneous in all the longitudinal sections, still indications were there of inversion base progressively raising from west to east and the inversion strength weakening in the sections 50°E to 75°E.

5·3. *At the stationary location 10°N, 60·2°E*

Fig. 17 gives details of inversion layer in the two spells one from 1 to 7 June 1973, when unstable conditions prevailed, and the other from 27 June to 4 July 1973 when stable or near stable conditions generally prevailed. There were practically no inversions in the spell I which was an active rainfall period over India. In the spell II there was an inversion layer in each of the ascent. The base of the inversion was however always above 1 km, mostly around 1·8 km. As already mentioned there was very weak rainfall activity over India during this spell.

6. Conclusions

6.1. *Summary of results*

The ISMEX-73 data along the equator and along 10°N in the Arabian Sea were studied for bulk layer estimates of boundary layer variables based on a numerical scheme by Deardorff. It was found that the buoyance effects were more

predominant in May, compared to June when mechanical processes became significant. Generally unstable conditions ($\theta_{vs} > \theta_{vm}$) prevailed in most cases. There were practically no inversions along the equator. Inversions were observed along 10°N and the data indicated that the inversion base became higher and the inversion strength weaker downstream from 50°E to 75°E. Observations at a stationary location 10°N, 60·2°E in two spells in June corresponding roughly to an active rainfall and a weak rainfall period over India were studied. The active rainfall spell boundary layers (*i*) were inversion free, (*ii*) had saturated mixed layers on many occasions, (*iii*) had always large positive sea-air virtual temperature difference, (*iv*) had larger specific humidity values compared to the boundary layers in the weak rainfall spell, which, (*i*) were characterised by inversions, (*ii*) had small sea-air virtual temperature values which were often negative, (*iii*) had sea surface virtual temperature values lower by about 2° in the average compared to the values in the active rainfall period, (*iv*) had larger values of wind speed and friction velocity compared to the active rainfall spell.

6·2. *Suggested future study*

The sea surface virtual temperatures decreased by 2° from May to June with the increase of wind speed. It is also evident from the data at 10°N, 60·2°E that the sea surface virtual temperatures were lower during the weak rainfall period over India, by about 2° compared to the values in the active rainfall period. It appears that the air temperatures had a process of adjustment to a lower value for a small positive sea-air temperature difference when the wind speed was increasing. During the period of adjustment the virtual air temperatures were often found higher than the sea surface virtual temperatures, a condition unfavourable for the production of turbulent kinetic energy and transport processes from the sea surface. There are many physical processes that influence the sea surface temperatures but the extent to which they are important depend on the time-scale considered. One of the influences is the modification of the depth of the mixed layer below the sea surface (analogous to the atmospheric mixed layer) with the scales of the order of days. Continued wind action agitates the upper layer and cooler water is entrained from below. If w_* is a the friction velocity in the water $[= (\rho_a/\rho_w)u_* \sim u_*/30]$ where ρ_a and ρ_w are air and water density, $\delta\rho$ is the density jump at the thermocline (analogous to the atmospheric inversion) across which the entrainment takes place, Kato and Phillips (1969) have shown from simple considerations :

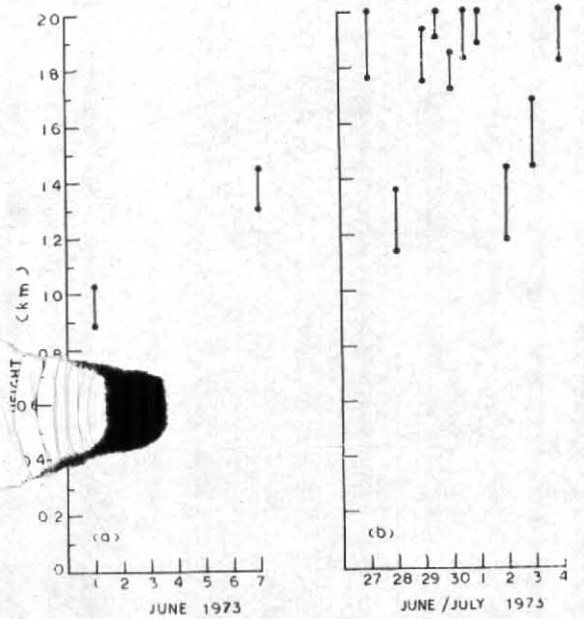

Fig. 17. Inversion layer at 10°N, 60·2°E

$$\frac{dh}{dt} \approx 2{\cdot}5 \ \frac{\rho_w \ w_*^3}{g \ \delta\rho \ h} \qquad (6.1)$$

$$\frac{dT}{dt} \approx -2{\cdot}5 \ w_*^3/(g \ \alpha \ h^2) \qquad (6.2)$$

where α is the thermal coefficient of expansion. From the oceanographic data of *Shokalaisky* which mainly cruised along 10°N the values of the height of the oceanic mixed layer h were found to have deepened from 30 m to 70 m from spell I to spell II. This amounts to a decrease of 2° in the sea surface temperature values in a day from spell I to spell II from (6·2) for $w_* \approx 1{\cdot}7$ cm corresponding to the observed u_* value of 50 cm. Though a comprehensive general circulation ocean-atmosphere model will be necessary to study these aspects in depth, still a single point time-dependent model of the upper ocean (Denman 1973) can be utilised for study as an initial value problem. The external parameters to be prescribed for predicting the ocean mixed layer height h and temperature T_s will be the solar radiation R with an extinction coefficient γ to assess the amount of R reaching the depth beneath the ocean, B the back radiation, τ_s the wind stress at the ocean surface, turbulent heat flux and the temperature gradient at the thermocline. This will be the subject for a future study.

Acknowledgement

The author is thankful to Dr. P. K. Das for suggesting the study and for his encouragement, to Mr. Man Mohan Srivastava for collection of data and to Mr. Hari Kishan for preparing the diagrams.

REFERENCES

Augstein, E., Shmidt, H. and Ostapoff, F.	1974	*Bound. Layer Met.*, **6**, pp. 129-149.
Bunker, A.	1965	Proc. Symp. IIOE, Bombay, pp. 3-16.
Businger, J. A.	1966	Transfer of momentum and heat in the planetary boundary layer. Proc. Symp. Arctic heat budget and atmospheric circulation California, Res. Memo. RM-5233-NSF Rand Corp. Santa Monica, Calif., pp. 305-333.
Businger, J. A., Wyngaard, J. C., Izuni, Y. and Bradley, E. F.	1971	*J. atmos. Sci.*, **28**, pp. 181-189.
Charnock, H.	1955	*Quart. J. R. Met. Soc.*, **81**, pp. 639-640.
Deardorff, J. W.	1970 (a)	*Geophys. Fluid Dyn. J.*, **1**, pp. 377-410.
	1970 (b)	*J. atmos. Sci.*, **27**, pp. 1209-1211.
	1972 (a)	*Ibid.*, **29**, pp. 91-115.
	1972 (b)	*Mon. Weath. Rev.*, **100**, pp. 93-106.
Denman, K. L.	1973	*J. phys. Oceanogr.*, **3**, 173-184.
Jambunathan, R. and Ramamurthy, K.	1974	*Indian J. Met. Geophys.*, **25**, pp. 403-410.
Kato, H. and Phillips, O. M.	1969	*J. Fluid Mech.*, **37**, pp. 643-655.
Kitaigorodskii, S. A. and Volkov, Y. A.	1965	*Izvestia Atmos. Oceanic Phys.*, **9**, pp. 973-988.
Melgarejo, J. W. and Deardorff, J. W.	1974	*J. atmos. Sci.*, **31**, pp. 1324-1333.
Monin, S. A. and Oboukhov, O. M.	1954	*Trudy geofiz. Inst.*, **24**, pp. 163-187.
Moss, M. S. and Rosenthal, S. L.	1975	On the estimation (From bulk data)of boundary layer variables and cloud mass flux in mature hurricanes. NOAA Tech. Memo ERL WMPO-23, 36 pp.
Pant, M. C.	1978	*Indian J. Met. Hydrol. Geophys.*, **29**, p. 88.
Pond, S., Fissel, D. B. and Paulson, C. A.	1974	*J. Bound. Layer Met.*, **6**, pp. 333-339.
Roll, H. U.	1965	*Physics of the marine atmosphere*, New York Academic Press, 426 pp.
Zilitinkevich, S. S. and Deardorff, J. W.	1974	*J. atoms. Sci.*, **31**, pp. 1449-1452.